Published in final edited form as:

Curr Biol. 2017 August 07; 27(15): 2357–2364.e5. doi:10.1016/j.cub.2017.06.037.

Two-element transcriptional regulation in the canonical Wnt pathway

Kibeom Kim[1,†], **Jaehyoung Cho**[1,†], **Thomas S. Hilzinger**[1,†,‡], **Harry Nunns**[1], **Andrew Liu**[1], **Bryan E. Ryba**[2], and **Lea Goentoro**[1,*,§]

[1]Division of Biology and Biological Engineering, California Institute of Technology, Pasadena, CA 91125

[2]Department of Physics and Department of Molecular Biology, University of California, San Diego, CA 92093

Summary

The canonical Wnt pathway regulates numerous fundamental processes throughout development and adult physiology, and is often disrupted in diseases [1, 2, 3, 4]. Signal in the pathway is transduced by β-catenin, which in complex with Tcf/Lef, regulates transcription. Despite the many processes that the Wnt pathway governs, β-catenin acts primarily on a single cis-element in the DNA, the Wnt-Responsive Element (WRE), at times potentiated by a nearby Helper site. In this study, working with *Xenopus*, mouse, and human systems, we identified a cis-element, distinct from WRE, that β-catenin and Tcf act on. The element is 11-bp long, hundreds of bases apart from WRE, and exhibits a suppressive effect. In *Xenopus* patterning, loss of the 11-bp negative regulatory elements (11-bp NREs) broadened dorsal expression of *siamois*. In mouse embryonic stem cells, genomic deletion of the 11-bp NREs in the promoter elevated *Brachyury* expression. This reveals a previously unappreciated mechanism within the Wnt pathway, where gene response is not only driven by WREs, but also tuned by 11-bp NREs. Using EMSA and Chip, we found evidence for the NREs binding to β-catenin and Tcf – suggesting a dual action by β-catenin as a signal and a feedforward sensor. Analyzing β-catenin Chip-Seq in human cells, we found the 11-bp NREs co-localizing with WRE in 45–71% of the peaks, suggesting a widespread role for the

*Corresponding author: goentoro@caltech.edu.
†These authors contributed equally to the work.
‡Current address: PricewaterhouseCooper LLP, Chicago, IL 60654
§Lead Contact

Author Contributions

J.C., T.S.H., K.K., A.L., B.E.R. and L.G. designed experiments, performed experiments, and performed data analysis. H.N. performed modeling analysis, contributed to data analysis, and wrote the model supplement. K.K. and L.G. wrote the manuscript.

DATA AND SOFTWARE AVAILABILITY.

The full sequence of the 3kb *siamois* promoter will be deposited to Pubmed. Constructs generated in the study are available upon request.

KEY RESOURCE TABLE.

Table provided in a separate file.

Methods S1. **Modeling analysis of incoherent feedforward loop.** This analysis describes how IFFL can produce different gene response dynamics, and how inclusion of an IFFL downstream the Wnt pathway can recapitulate endogenous gene regulation.

mechanism. This study presents an example of a more complex cis-regulation by a signaling pathway, where a signal is processed through two distinct cis-elements in a gene circuitry.

Keywords

Canonical Wnt pathway; β-catenin; Tcf; cis-regulation; gene transcription; *siamois*; *Brachyury*; *Xenopus*; mouse embryonic stem cells

Results

We started with a previously reported discrepancy between the endogenous gene and TopFlash reporter expression (Figure 1B–D) [5]. Wnt signaling in early *Xenopus* blastulas activates dorsal regulators, including *siamois* and *Xnr3*. Treating the embryos for 5–10 minutes with 300 mM lithium is known to inhibit GSK3β [6], stabilize β-catenin [7], and dorsalize the embryos (Figure 1B–C) [8, 9]. We observed, however, that embryos treated with moderate doses of lithium (150 and 200 mM) largely retained a wild-type level of *siamois* and *Xnr3* expression (Figure 1C, see red arrows), and developed into wild-type tailbuds (Figure 1B). More strikingly, despite absence of marked phenotypic effects, the embryos showed increased β-catenin level (Figure 1D, see red arrows). Similar lack of embryo phenotypes despite increased β-catenin level was observed with other perturbations to the Wnt pathway, including injection of *Axin1* and *GBP* mRNA. This led us to assay the TopFlash reporter, a commonly used reporter of Wnt signaling driven by a tandem repeat of WREs, to test whether the increased β-catenin was transcriptionally active. Indeed, the TopFlash reporter also showed increased activity at moderate doses of lithium (Figure 1D, red arrows). Therefore, even though the TopFlash reporter faithfully tracked the rise of β-catenin level, the contrasting wild-type expressions of the endogenous genes suggest a missing mechanism beyond WRE. It is notable that β-catenin itself, as a central regulator in the pathway, did not correlate with the target gene expression but tracked the extent of the perturbations, hinting at a possible role for β-catenin in the missing regulation.

An 11-bp negative regulatory element is necessary for dorsal specification of *siamois*

To locate the missing regulation, we focused on *siamois* [9, 10, 11]. Three WREs are found within 500 bp upstream of *siamois*, and are necessary for *siamois* activation (Figure 2A) [10, 11]. We built a luciferase reporter using a 3kb fragment of *siamois* promoter (pSia). We confirmed that 3kb pSia-luc mimics the temporal expression of *siamois*, beginning at mid-stage 8 and reaching steady state by stage 10. Reported here is the luciferase expression at early stage 10, reliably identified by the onset of dorsal lip formation.

We perturbed the GSK3β activity in a dose-response manner as described earlier. We found that the 3kb promoter recapitulated the endogenous *siamois* response, preserving wild-type expression at 150 mM LiCl (Figure 2B). By contrast, an 848bp fragment of *siamois* promoter that still contains the three WREs responded readily to perturbations (Figure 2C). To examine the spatial regulation of these promoter fragments, we tested lacZ reporters. Indeed, even though 3kb and 848bp-lacZ retained dorsal expression, the 848bp fragment showed expanded expression (Figure 2C–D inset). The missing regulation in the 848bp

fragment was especially revealed when a moderate lithium dose was applied: the 3kb pSia-lacZ preserved dorsal expression at 150 mM LiCl, whereas the 848bp pSia-lacZ readily expanded.

Therefore, a suppressive, distal element located between 848bp and 3kb is necessary for the dorsal specification of pSia expression. Using the differential response at 150 mM lithium as a readout, we performed a promoter bashing screen to locate the element. Halving to 1.3kb preserved wild-type reporter expression, as did further truncations up until 963bp (Figure 2D, F). Loss of suppression at 150 mM LiCl was finally observed with truncation to 952bp, and with subsequent shorter constructs (Figure 2E, F). This analysis identified a suppressive element at 1kb upstream from *siamois*, with most activity centered on an 11-bp between 963 and 952bp (Figure 2G).

The 11-bp negative regulatory element (11-bp NRE) is AT-rich, 5'- CTG TTA TTT AA -3'. To further characterize the 11-bp NRE, we performed a mutagenesis analysis. With the 1.3kb promoter fragment, we mutated the 11-bp NRE one base at a time (*i.e.*, purine into pyrimidine, or vice versa). We found that the majority of single-base alterations affected the response, with the largest effect produced by a single-base mutation on the 11th nucleotide, which recapitulated the effect of deletion of the 11-bp NRE (Figure 2H). Finally, the 11-bp NRE is sufficient to recapitulate the suppression. Inserting the 11-bp NRE to 848bp promoter (Figure 2F) rescued the wild-type expression. The same effect was observed when the 11-bp NRE was pasted to even shorter promoters (Figure S1). These results suggest that regulation of *siamois* not only requires WREs, but also a suppressive 11-bp NRE.

The 11-bp NRE interacts with Tcf

Next, we set out to find the factors that bind to the 11-bp NRE using EMSA (Figure 3A, B). As the protein source, we used the high-speed supernatant of *Xenopus* egg extracts. We reasoned that the binding factor(s) must be maternal, as Wnt signaling begins in early blastula before zygotic transcription [12, 13]. As the DNA probe, we synthesized a 30-bp double stranded oligomer containing the 11-bp NRE, flanked by the endogenous sequence. As a control for the probe, we used the strongest mutant with an A–>C switch at the 11th nucleotide (m11 mutant; Figure 2H).

We observed specific binding to the 11-bp NRE in the EMSA (Figure 3C). The band was competed away when excess, unlabeled DNA probe was added (Figure 3C, lanes 3–4). The band was competed away much less effectively when excess, unlabeled m11 mutant probe was used (Figure 3C, compare lanes indicated by blue arrows). The specific band was reproducible across batches of extracts, despite variation in nonspecific binding patterns and the amount of competitors needed (Figure 3C).

Having the specific EMSA activity, we proceeded to identify the binding factor(s) by testing some known transcription factors. Lacking good antibodies to these factors in *Xenopus*, we tested if the DNA binding sites of the factors would compete with the EMSA band. Binding sites of various transcription factors, *e.g.*, CREB, p53, NF-κB, AP-1, failed to compete significantly (Figure S2A). Unexpectedly, the one DNA fragment that competed away the EMSA band was the WRE itself (Figure 3D). The specific band was competed away when

excess, unlabeled WRE probe was added (Figure 3D, lanes 5–6) – to a similar extent as it was competed away by excess, unlabeled wild-type probe (Figure 3C, lanes 3–4). By contrast, a negative control probe, carrying two mutations that destroy binding of the Tcf protein (*i.e.*, FopFlash construct) [14], competed much less effectively (Figure 3D, lanes 7–8, see blue arrows).

The competition by WRE suggests that Tcf proteins bind to the 11-bp NRE. Indeed, XTcf3 antibodies, raised against an N-terminal (XTcf3n) and C-terminal fragment (XTcf3c) [15], competed away the specific band (Figure 3E). These results suggest that a Tcf/Lef protein binds the 11-bp NRE, and that XTcf3 is the predominant binder in our *in vitro* assay.

The 11-bp NRE interacts with β-catenin

The binding of Tcf protein to the 11-bp NRE raises questions on the binding partner, as Tcf does not usually act alone [4]. The binding of Tcf to the 11-bp NRE is also interesting in light of our earlier findings (Figure 1) that β-catenin intriguingly tracks the extent of perturbations, motivating us to test the roles of β-catenin.

We found that adding polyclonal β-catenin antibody to the EMSA reaction produced a strong supershift, and a weak downshift smear (Figure 3F). To further confirm the binding of β-catenin, we performed binding assay using purified recombinant *Xenopus* β-catenin and Tcf3 (Figure S2B). As expected, Tcf3 alone produces a smear signal, suggesting an unstable binding. A strong, sharp band was observed in the presence of both Tcf3 and β-catenin.

To test if β-catenin acts on the 11-bp NRE in the *siamois* promoter *in vivo*, we performed chromatin immunoprecipitation in the embryos (Figure 3G). We collected embryos at stage 10, when *siamois* expression is at peak. We observed a strong signal indicating β-catenin binding in the 11-bp region. In the same experiment, as expected, β-catenin binding was also detected from the WRE region in the *siamois* promoter. As a negative control, negligible signal was detected with IgG antibody and from *siamois* or *ODC* coding regions. These results suggest that the 11-bp NRE, required for *siamois* regulation, interacts with β-catenin and Tcf.

The 11-bp NRE is present in the promoter of more target genes

Beyond *siamois*, might the 11-bp NRE regulate other Wnt target genes? At first, we found no results looking for the exact 11-bp sequence in other *Xenopus* targets. However, examining the *siamois* promoter closely, we identified two sites with a sequence pattern similar to that of the 11-bp NRE (Figure 4A–B), a G/C cap, followed by 8 A/T's – with an occasional C/G in the 5th position. All 11bp-like elements competed with the WRE (Figure S3A). Hence, three 11-bp NREs are present in the *siamois* promoter, although losing the distal one is sufficient to disrupt the suppression. Following this lead, we searched for a similar sequence pattern in other known direct Wnt targets in *Xenopus*. We found candidate 11-bp NREs in the promoter of *Xnr3* and *engrailed* (Figure 4B). The predicted 11-bp NREs in *Xnr3* and *engrailed* produced a specific EMSA band, which was shifted by polyclonal β-catenin antibody (Figure S3B).

The 11-bp NRE regulates *Brachyury* expression in mouse embryonic stem cells

With the predictive sequence pattern (Figure 4C), we investigated if 11-bp NRE is present in mammals. We examined promoters of known direct Wnt targets in mouse embryonic stem cells (mESC). We identified several candidates, including some in the promoters of well-characterized Wnt targets, such as *Brachyury* (*T*), *Axin2*, and *Cdx4* (Figure 4B). EMSA assay confirmed that these 11-bp NREs produced a specific band that was shifted by β-catenin antibody (Figure S3C).

To test whether the 11-bp NREs function in regulation of mammalian Wnt targets, we examined *T* regulation. *T* promoter has two WRE sites, at 191 and 273 bp upstream of the transcription start site (Figure 4D) [16]. *T* is an early marker of mesoderm differentiation. Basal expression of *T*, present in a fraction of stem cell population [17], is activated by endogenous secretion of Wnt proteins [18] and marks the early mesoderm-committed (EM) progenitors [17].

We identified two candidate 11-bp NREs, at 999 and 1613 bp upstream from the transcription start site (Figure 4D). To test whether the 11-bp NREs interact with β-catenin *in vivo*, we performed chromatin immunoprecipitation using β-catenin antibody. We observed signal from the proximal 11-bp NRE (Figure 4E). As positive control, strong signal was also observed from the −273bp WRE (Figure 4E). As negative controls, almost tenfold lower signal was observed using mouse IgG antibody, and negligible signal from the exon 2 region of *T*. We observed much lower signal from the distal NRE, suggesting the proximal one as the dominant NRE in the *T* promoter.

To test the roles of the 11-bp NREs in *T* regulation, we used Crispr/Cas9 to delete the 11-bp NREs from the endogenous promoter of *T*. Four sequence-verified *T*Δ11bp clones were then assayed for *T* expression by qRT-PCR. We observed that *T*Δ11bp clones showed significantly higher expression levels of *T* than the wild type cells (Figure 4F), suggesting increased EM progenitors. As a control, four wild-type clones that underwent blank transfection and clonal selection showed no significant change of *T* expression. These results suggest that balanced regulation of *T* in mESC require 11-bp NREs as well as the WREs.

The 11-bp NRE is prevalent in β-catenin Chip-Seq in human cells

Finally, equipped with the criterion of 11-bp NRE gathered across several Wnt direct targets (Figure 4C), and one confirmed with binding and functional assays (Figure 2,3, 4E–F), we asked whether 11-bp NREs are present more widely across Wnt target genes. To address this question, we analyzed β-catenin Chip-Seq datasets from human cells [19, 20]. We found significant enrichment of 11-bp NREs in β-catenin peaks from HEK293T (p-value: 2.58 e–31) and HCT116 cells (p-value: 4.24e–12). Multiple 11-bp NREs were often predicted within the β-catenin-bound fragments. We found significant co-localization of 11-bp NREs with WRE: of the 2818 β-catenin peaks that contain WRE, 71% also contain 11-bp NREs in in HEK293T cells (Figure 4G), and 45% do so in HCT116 cells (Figure S4). Our analysis also indicates a significant fraction of β-catenin-bound fragments that contains 11-bp NREs only (Figure 4G), suggesting that the 11-bp NRE may have more functions beyond what we found here.

Discussion

We found an 11-bp NRE that β-catenin and Tcf act on in the promoters of many Wnt target genes. The 11-bp NRE is necessary for *siamois* regulation in *Xenopus* embryos and *Brachyury* regulation in mouse embryonic stem cells. Our study suggests a new model of gene regulation in the Wnt pathway, where signal in the pathway not only activates target genes through WRE, but also in some contexts, tunes expression of the genes through a distinct 11-bp NRE. (Figure 4I). Interestingly, although multiple NREs are present in *siamois* and *T* promoter, there seems to be a dominant one that mediates suppression. The Chip data in *T* promoter suggests that the other NRE binds less strongly to β-catenin and therefore may play subtler roles. In *Drosophila*, it was found that Wnt signaling represses Ugt36Bc and TiG genes through a WGAWAW site that binds to β-catenin [14]. Our finding identifies a distinct repressive site in vertebrates, and one that implicates a different role for β-catenin, where it acts in opposite manner in the same promoter, as an activator through WRE and a suppressor through the 11-bp NRE. With regard to Tcf, our finding can be consistent with models in the field, where the same or distinct Tcf proteins may specialize as an activator or a repressor [4].

A circuit where the input activates the output, and at the same time suppressively tunes the output, is known in engineering as the incoherent feedforward loop (IFFL). Such a circuit has been found in transcriptional networks of bacteria, yeast, and human cells [22–25]. While these analysis focused on protein-protein interactions, an interesting aspect of the IFFL we found in the Wnt pathway is its implementation through multiple cis-elements. We know of one other instance where a regulator works through multiple cis-elements in an IFFL mode, in the regulation of porin OmpF in *E. coli* [26].

More generally, IFFL belongs to a class of recurring strategy in biological systems, where a biological molecule is used in a paradoxical manner (27). Paradoxical circuits, and the incoherent feedforward circuit specifically, moreover, are versatile circuits. By tuning the relative strengths and time scales of the activation and repression arm, an incoherent feedforward circuit can generate a sustained, net activation – but beyond that, also a net repression, a temporal pulse, response acceleration, band-pass filtering, and fold-change detection (see Methods S1, as well as refs. [28–34]). Moreover, inclusion of an IFFL downstream the Wnt pathway can explain how the endogenous gene response remains wild type despite perturbations, either by acting as an amplitude filter (if the timescales of activation and repression are similar) or fold-change detector (if the repression is slow and strong) (see Methods S1). Although it is difficult presently to estimate the relative affinities of the two sites, an extract system combined with sophisticated methods such as SPR could be a next approach. It would also be interesting to investigate whether different co-factors or chromatin modifiers are recruited by β-catenin to the 11-bp NRE. Thus, the finding of the 11-bp NRE not only suggests a different model of gene regulation in the Wnt pathway, and one that implicates a function for β-catenin as a feedforward sensor, but also provides a plausible mechanism by which gene regulation by β-catenin and Tcf can generate more versatile dynamics across contexts.

STAR Methods

CONTACT FOR REAGENT AND RESOURCE SHARING

Further information and requests for reagents may be directed to, and will be fulfilled by the corresponding author Lea Goentoro (goentoro@caltech.edu).

EXPERIMENTAL MODEL AND SUBJECT DETAIL

Xenopus laevis—Experiment protocols were approved by the Institutional Animal Care and Use Committees and performed in accordance with NIH guidelines. Female and male mature pigmented *Xenopus laevis* were obtained from Nasco (female LM00535MX, male: LM00715MX). The *Xenopus* is housed in an aquarium system (Aquannering) equipped with UV light, with automated control of conductivity, pH, and temperature. The animals are daily fed with Nasco frog brittle (Nasco cat# SA05961(LM)MX). Female frogs rested for 3–4 months between egg collection. Male frogs were euthanized for testis dissection.

Mouse embryonic stem cells (mESC)—E14 mESC (E14Tg2a.4) were obtained from Mutant Mouse Regional Resource Centers (015890-USCD). The mESC was cultured on 0.1% gelatin coated plates with Glasgow's MEM supplemented with 1000 U/mL LIF (Millipore, ESG1106), 10% ES-certified FBS (Thermo Fisher 16141061), non-essential amino acids, and L-glutamine. To confirm the identity of the mESC, we performed differentiation assay, confirmed the expected changes in cell morphology, and verified expression of pluripotency and differentiation markers using qRT-PCR, including *Nanog, Oct4, Brachyury, Flk1, Myf5, Gata4, Sox17, Pax6, Otx2.* We confirmed the purity of the culture by performing mycoplasma testing.

METHOD DETAILS

***Xenopus in vitro* fertilization—**was performed according to [35]. Testes were isolated from male *X. laevis* and stored in 1× Marc's Modified Ringer (MMR) with 50 μg/ml gentamicin for up to two weeks. Ovulation was induced in female *X. laevis* by injection of 600–800U human chorionic gonadotropin (HCG) 14–16 hours prior to egg collection. Eggs were fertilized by incubation in a sperm solution in 0.1×MMR for 30 minutes. Fertilized eggs were dejellied in 20 mg/ml cysteine, pH 8.0 in 0.1×MMR for 2–5 minutes. Embryos were reared in 0.1×MMR at 14°C.

DNA constructs—3kb fragment of the *siamois* promoter [10] was inserted into pGL4.12 (Promega, E6671) using KpnI and BglII. For promoter analysis, the desired length of a promoter fragment was amplified out, and cloned into pGL4.12 using KpnI and BglII. For the rescue experiments, the desired length of a promoter fragment was amplified out with the 11-bp sequence added on the 5' end, with 5bp of endogenous sequence 3' to the 11-bp NRE included as a spacer. For mutagenesis analysis, single-base mutation was performed on 1.3 kb pSia-luc using QuikChange II (Agilent Technologies, 200523).

Embryo microinjection—Needles for microinjection were made from capillary tubing (Borosil 1.2mm × 0.9mm ID, FHC Inc, 30-31-0) pulled using Flamming/Brown micropipette puller (Sutter Instrument, P-97). The needle was calibrated to produce a 10nl

ejection volume. Calibrated needles were attached to a microinjector (Warner Instruments, Picoliter Microinjector PLI-100A) and filled with the DNA construct solution. Embryos were collected at 4-cell stage, and placed in 5% Ficoll/0.1×MMR. Each cell in the embryos was injected with 10nl solution on the equator for a total of 4 injections per embryo. Injected embryos were reared in 0.1× MMR.

Lithium treatment—Treatment with lithium chloride (Sigma, L4408) was performed when the embryos were at 32-cell stage, by incubating the embryos for 5 min in 0.1× MMR with 0 mM, 150 mM, or 300 mM LiCl. Embryos were subsequently thoroughly washed, let develop further in 0.1× MMR, and harvested at the appropriate stage for different assays.

Dual luciferase assay—Embryos were injected at 4-cell stage with a total of 100 pg/mL pSia-luc and 25 pg/mL modified pRL-TK (Promega, E2241). The modified pRL-TK has the Rluc gene replaced with the hRlucCP from pGL4.84 (Promega, E7521), which is the destabilized version of Rluc and produces quicker and stronger expression than its stable counterpart. Dual luciferase assay was performed using the Promega system (E1960). Three to four pools of 10 embryos at stage 10 were collected from each sample and lysed in 50 μl of Passive Lysis Buffer. 5–10μl of cleared lysate was analyzed on a Victor X plate reader (PerkinElmer). For each biological replicate, 2–3 technical replicates were measured. The ratio of firefly to renilla luciferase activity (Luc/Ren ratio) was calculated for each data point, and averaged across the technical replicates.

β-galactosidase assay—*Xenopus* embryos were injected with 3kb or 848bp pSia-LacZ at 4-cell stage, treated with lithium for 5 minutes at 32- to 64-cell stage, and fixed at stage 10. To visualize the promoter activity, expression of β-galactosidase was detected by x-gal staining following the manufacturer's procedure (Thermo Fisher, K1465-01). 30 embryos/tube were incubated in the fixing buffer for 30 minutes on a nutator at room temperature, rinsed twice with 1× PBS + 2 mM $MgCl_2$, and stained with 0.5 mL of staining buffer at 37°C in the dark until the stain develops. Afterward, the embryos were washed twice with 1× PBS, twice with methanol, and photographed.

***Xenopus* extract—**preparation was performed according to [36] with modifications. Female *X. laevis* frogs were injected with 50 units of PMSG 2 days prior and 600–800U HCG 16 hours prior to egg collections. Each frog was placed in a container with 3–4L of 1×MMR. The next day, eggs were rinsed, examined for quality, and dejellied in 10 mM DTT / 50mM Hepes pH 8.2. Dejellied eggs were rinsed in Wash Buffer (20 mM Hepes pH 7.9, 2 mM MgCl2, 0.1 mM EDTA pH 8, 100 mM KCl), transferred to Extraction Buffer (Wash Buffer, 1mM DTT, 10 μg/mL each of leupeptin, chymostatin and pepstatin A). Eggs were packed by quick centrifugation, the excess liquid removed, and crushed by centrifugation at 10,000g for 15 minutes. The crude supernatant was diluted to ~10mg/mL, and then cleared further with centrifugation at 100,000g for 1 hour. The high speed supernatant was used for EMSA analysis.

Electric Mobility Shift Assay (EMSA)—Double stranded DNA probes were synthesized from IDT and labeled at the 5' end of one strand with IR680 or IR800 dye. 4 μl of *Xenopus* egg extract was added to a 20 μl total reaction mixture containing 20 mM HEPES pH 7.9, 50

mM KCl, 10 mM MgCl2, 1 μg/ml poly(dI-dC), 4% Ficoll 400, and incubated for 30 min on ice. 1 μl of labelled probe DNA (50 fmol) was then added, and the reaction was incubated for another 2 hours to overnight on ice. The whole binding reaction was loaded onto a 4% or 6% native DNA retardation gel with 1× TGE buffer (Novex EC6058BOX, Invitrogen). Gels were run at 115 V at 4°C in 1× TGE buffer for 1.75 hr (before the actual run, the gels were pre-run for an hour). For the probe competition assays, the reaction mixture was pre-incubated with unlabeled dsDNA competitors for 30 minutes, before adding the labeled probe. For the antibody competition assay, specific antibodies were pre-incubated with the reaction mixture for 1.5 hrs before addition of the labeled probe. The gel was imaged directly with the LiCOR Odyssey Imager.

Purification of recombinant Xβ-catenin and XTcf3—Xβ-catenin-His9 or GST-XTCF3-His9 in pETKatN10 were expressed and purified from *E. coli* BL21 (DE3) (EMD, 69450). For protease inhibitors, we used 1× cOmplete EDTA-free protease inhibitor (Roche, 11873580001). Transformed cells were cultured with shaking at 37°C until OD600 is 0.4, and then chilled on ice for 20 min. Protein expression was induced with 0.4 mM IPTG for 3hrs at 25°C. Cell pellets were suspended in lysis buffer (1× PBS, 500 mM NaCl, 0.5% Triton X-100, 0.1% BSA, 1% glycerol, 5 mM DTT, protease inhibitors) and sonicated 5×10 seconds at 30% output. Crude cell extracts were centrifuged for 20 min. GST affinity purification: clarified extract was incubated with glutathione sepharose beads (GE Healthcare, 17-0756-01) for 2.5 hrs at 4°C. Beads were washed with wash buffer (1× PBS, 500 mM NaCl, 0.5% Triton X-100,1% glycerol, 5 mM DTT, protease inhibitors) for 30 min at 4°C. GST-XTCF3-His9 was eluted with elution buffer (20 mM reduced glutathione, 50 mM Tris HCl pH 9.5, 150 mM NaCl, 1 mM DTT, 0.1 % Triton X-100), dialysed against dialysis buffer (50 mM Tris-HCl pH 7.4, 300 mM NaCl, 1 mM DTT, 0.01% TritonX-100) using Slide-A-Lyzer 10,000 MWCO (Thermo Scientific), and concentrated with Vivaspin2 (VIVAproducts). His-tag affinity purification: the partially purified fraction from GST-affinity purification for GSTXTCF3-His9 or bacterial lysate expressing Xβ–catenin-His9 was applied to Ni-NTA column, and incubated with gentle rotation for 3 hrs at 4°C. Unbound proteins were removed by gravity-flow and washed 3 times with wash buffer (1× PBS, 20 mM Imidazole, protease inhibitors). Target proteins were eluted with elution buffer (1× PBS, 250 mM Imidazole, pH 7.4) with gentle rotation at 4°C, 30 minutes, concentrated and buffer changed to 10 mM HEPES-KOH (pH 7.9) with Amicon Ultra-15 10,000 MWCO (EMD Millipore, UFC901008).

Chromatin immuniprecipitation—*Xenopus* embryos. Embryos at stage 10 were fixed and crosslinked with 1% formaldehyde/PBS for 1 hr. Crosslinking was stopped with 125 mM glycine/PBS. Fixed embryos were transferred to 600 μl of cold RIPA buffer (50 mM Tris-HCl, pH 7.4, 1% NP-40, 0.25% Na-Deoxycholate, 150 mM NaCl, 1 mM EDTA, 0.1% SDS, 0.5 mM DTT, Roche protease inhibitor cocktail), homogenized with a pestle, and then let sit on ice for 15 min. The chromatin was pelleted at 14,000g for 10 min at 4°C. The pellet was resuspended in 650 μl of cold RIPA buffer, sonicated for 10 rounds of 20 second bursts with 30% output and 45 second intervals for each round. The supernatant was cleared with 14,000g for 10 min at 4°C, and incubated with BSA-blocked protein G agarose beads (50 μl) for 2 hours to reduce non-specific binding. The pre-cleared supernatant was incubated with 1

μg of Xβ-catenin antibody or control IgG pre-coated protein G beads (50 μl per each condition) overnight at 4°C with mixing. The beads were washed three times each with wash buffer A (20 mM Tris-HCl, pH 8.0, 0.1% SDS, 1% Triton X-100, 2 mM EDTA, 500 mM NaCl) and wash buffer B (10 mM Tris, pH 8.0, 0.25M LiCl, 1% NP-40, 1% Na-Deoxycholate, 1 mM EDTA). The washed beads were treated with DNase-free RNase A in 10 mM Tris-HCl, pH 8.0 for 1 hr, and then washed twice with 1 ml of TE (10 mM Tris, p8.0, 1 mM EDTA). To elute the immune-complexes, the beads were incubated in 250 μl of TES buffer (50 mM Tris-HCl, pH 8.0, 10 mM EDTA, 1% SDS) at 65°C for 10 min with vigorous vortexing every 2 min. Crosslinking was reversed by heating at 65°C overnight with 0.5 mg/ml Proteinase K, 0.1% SDS in PBS. The released DNA was purified and analyzed by PCR. **mESC.** Cells were to grown to 80% confluency on 10 cm plates, crosslinked with 1% formaldehyde/PBS for 10 minutes at 21°C. Crosslinking was stopped with 125 mM glycine/PBS and washed twice with PBS. Fixed cells were scraped and collected in 1 mL PBS with 10uL of 100× protease/phosphatase inhibitor cocktail (Thermo Scientific, 1861281). The cells were then centrifuged at 10,000 g for 10 minutes at 4°C and resulting pellet was frozen at −80°C. Nuclear fraction of the cells was isolated using a hypotonic lysis buffer (10 mM Tris-HCl, pH 7.5, 10 mM NaCl, 3 mM MgCl2, 0.3% NP-40, 10% glycerol) [37]. We then proceeded with Chip-IT kit (Active Motif, 53040), with the given protocol except that we used Dynabeads Protein G (Thermo Fisher, 10003D). Sonication performed at 40 cycles of 0.7s on / 3.3s off at 20% amplitude using Branson SFX 250 Sonicator to break down chromosomes into 0.1 – 0.3 kb fragments. For pulldowns, we used mouse β-catenin antibody (BD Transduction Laboratories, 610153) and normal mouse IgG (Millipore, 12–371B) as a control.

Crispr/Cas9 transfection in mESC—We obtained PX330 generously donated to Addgene by the Feng Zhang lab [38]. Into the PX330 plasmid, we inserted gRNA sequence targeting the *T* promoter, removed the Cas9 coding cassette, and inserted neomycin resistance cassette. To synthesize the donor plasmid for TD11-bp clones in mESCs, we used genomic prep of the cells to clone out 5' and 3' homologous arms in the *T* promoter. Another insert fragment was cloned from the genomic prep that included deleted 11-bp regions. The three fragments were integrated into a generic plasmid backbone using Gibson assembly (New England Biolabs, E2611S).

For transfection, 2.5×10^5 mESCs were plated on 24 wells and grown overnight. We used 400 ng of the modified PX330 plasmid, 150 ng of donor plasmid, 12 pmol Cas9 recombinant protein (IDT, 1074182) in Lipofectamine LTX with PLUS (Thermo Fisher, 15338100). The cells were transfected for 24 hours, transiently selected with neomycin for 5 days, dissociated into single cells, and grown as single clones.

RT-PCR—Total RNA from mESC was isolated with RNeasy extraction kit (Qiagen 74104). cDNA was synthesized using Quantitect RT (Qiagen 205311). Real-time RT-PCR was performed using Quantitect SYBR-Green kit (Qiagen 204143) using StepOnePlus RT-PCR System (Applied Biosystems). Primer sequences are as follow:

TBP Fwd	5’ - ACATCTCAGCAACCCACACA - 3’
TBP Rev	5’ - GTGAAGGGTACAAGGGGGTG - 3’
T Fwd	5’ - GCTTCAAGGAGCTAACTAACGAG - 3’
T Rev	5’ - CCAGCAAGAAAGAGTACATGGC - 3’

Position Frequency Matrix—Position frequency matrix was built by aligning 11-bp NRE sequences using enoLOGOS [39] (http://lagavulin.ccbb.pitt.edu/cgi-bin/enologos/enologos.cgi), and logos were plotted by relative entropy and weighted by alignment frequency.

Chip-Seq data analysis—β-catenin enriched peaks were called following the original authors’ protocols [19, 20]. In summary, β-catenin peaks for Chip-Seq on HEK-293T cells were called using the CisGenome package [40] using window size of 100, step size 25, maximum gap 200, active single strand filtering, and FDR cut off of 0.01. β-catenin peaks for Chip-Seq on HCT-116 cells were called using three peak calling programs-CisGenome, SISSRs [41], and WTD [42]. CisGenome peak calling was run using window size of 100 and FDR cut off of 0.01. SISSRs was run using window size of 20 bases with the FDR of 0.01. WTD was run with variable window size estimations and with FDR cut off of 0.01. Peaks called in all three programs were identified and used. For each enriched peak, 200bp or 1k bp of genomic sequence was isolated, and then repeat-masked using RepeatMasker 2.0 (http://www.repeatmasker.org/). Control sequences were obtained through random shuffles of the peak sequences, maintaining the nucleotide composition. Enrichment of WRE and 11-bp motifs in the peak regions was analyzed using MEME Suites AME (http://meme-suite.org/doc/ame.html) [43] and FIMO (http://meme-suite.org/doc/fimo.html) [44]. In AME, user provided motifs (WRE and 11-bp NREs) are scored on enrichment of the experimental sequences (Chip-Seq peaks) and compared to the shuffled control sequences. Statistical significance is calculated by Mann-Whitney U test. FIMO scans Chip-Seq peaks and returns all sequences that match user-provided motifs.

QUANTIFICATION AND STATISTICAL ANALYSIS

Statistical parameters including the number of biological and technical replicates, the definition of center, dispersion and precision measures (mean ± SEM or mean ± SD) and statistical significance are reported in the Figures and Figure Legends. Statistical significance is defined as when $p < 0.001$ by Student’s t test, and denoted by *** in figures.

Supplementary Material

Refer to Web version on PubMed Central for supplementary material.

Acknowledgments

We wish to dedicate this paper to Eric H. Davidson (1937–2015). His singular vision, commitment to truth, and unwavering intellectual rigour kept us all vigilant. His inspiring presence is deeply missed.

We thank Marc Kirschner, in whose lab the early part of this work was performed and for discussions afterward. We thank David Kimelman and Sergei Sokol for *siamois* promoter clones, Michael Klimkowsky for XTcf3 antibodies, Bil Clemons, Axel Müller, and Katrin Tiemann for pETKatN10 protein expression vector, and Hans Clevers, Jurian Schuijers, Michal Mokry, and Gregory Yochum for sharing their Chip-Seq data. We thank Ellen Rothenberg, Ray Deshaies, Christopher Frick, and Michael Abrams for discussions. This work was supported by the NIH New Innovator Award (1DP2OD008471) to L.G., NIH Training Grant (5T32GM007616-37) for H.N., and Caltech's SURF and Amgen Scholar to B.E.R.

References

1. Nusse R, Varmus H. Three decades of Wnts: a personal perspective on how a field developed. EMBO J. 2012; 31:2670–2684. [PubMed: 22617420]
2. Anastas JN, Moon RT. WNT signalling pathways as therapeutic targets in cancer. Nat. Rev. Cancer. 2013; 13:11–26. [PubMed: 23258168]
3. Loh KM, van Amerongen R, Nusse R. Generating cellular diversity and spatial form: Wnt signaling and the evolution of multicellular animals. Dev. Cell. 2016; 38:643–655. [PubMed: 27676437]
4. Cadigan KM, Waterman ML. TCF/LEF and Wnt signaling in the nucleus. Cold Spring Harb. Perspect. Biol. 2012; 4:1–23.
5. Goentoro L, Kirschner MW. Evidence that fold-change, and not absolute level, of β-catenin dictates Wnt signaling. Mol. Cell. 2009; 36:872–884. [PubMed: 20005849]
6. Klein PS, Melton DA. A molecular mechanism for the effect of lithium on development. Proc. Natl. Acad. Sci. 1996; 93:8455–8459. [PubMed: 8710892]
7. Schohl A, Fagotto F. β-catenin, MAPK and Smad signaling during early *Xenopus* development. Development. 2002; 129:37–52. [PubMed: 11782399]
8. Kao KR, Elinson RP. Dorsalization of mesoderm induction by lithium. Dev. Bio. 1989; 132:81–90. [PubMed: 2917698]
9. Lemaire P, Garrett N, Gurdon JB. Expression cloning of Siamois, a *Xenopus* homeobox gene expressed in dorsal-vegetal cells of blastulae and able to induce a complete secondary axis. Cell. 1995; 81:85–94. [PubMed: 7720076]
10. Brannon M, Gomperts M, Sumoy L, Moon RT, Kimelman D. A β-catenin/XTcf-3 complex binds to thesiamois promoter to regulate dorsal axis specification in Xenopus. Genes & development. 1997; 11(18):2359–2370. [PubMed: 9308964]
11. Fan MJ, Grüning W, Walz G, Sokol SY. Wnt signaling and transcriptional control of Siamois in *Xenopus* embryos. Proc. Natl. Acad. Sci. 1998; 95:5626–5631. [PubMed: 9576934]
12. Larabell CA, Torres M, Rowning BA, Yost C, Miller JR, Wu M, Kimelman D, Moon RT. Establishment of the dorso-ventral axis in *Xenopus* embryos is presaged by early asymmetries in beta-catenin that are modulated by the Wnt signaling pathway. J. Cell Biol. 1997; 136:1123–1136. [PubMed: 9060476]
13. Tao Q, Yokota C, Puck H, Kofron M, Birsoy B, Yan D, Asashima M, Wylie CC, Lin X, Heasman J. Maternal wnt11 activates the canonical wnt signaling pathway required for axis formation in *Xenopus* embryos. Cell. 2005; 120:857–871. [PubMed: 15797385]
14. Korinek V, Barker N, Morin PJ, van Wichen D, de Weger R, Kinzler KW, Vogelstein B, Clevers H. Constitutive transcriptional activation by a β-catenin-Tcf complex in APC−/− colon carcinoma. Science. 1997; 275:1784–1787. [PubMed: 9065401]
15. Zhang C, Basta T, Jensen ED, Klymkowski MW. The β-catenin/VegT-regulated early zygotic gene *Xnr5* is a direct target of SOX3 regulation. Development. 2003; 130:5609–24. [PubMed: 14522872]
16. Arnold SJ, Stappert J, Bauer A, Kispert A, Herrmann BG, Kemler R. Brachyury is a target gene of the Wnt/β-catenin signaling pathway. Mech of Dev. 2000; 91:249–258.
17. Suzuki A, Raya Á, Kawakami Y, Morita M, Matsui T, Nakashima K, Gage FH, Rodriguez-Esteban C, Izpisua Belmonte JC. Maintenance of embryonic stem cell pluripotency by Nanog-mediated reversal of mesoderm specification. Nat. Clin. Pract. Cardiovasc. Med. 2006; 3:S114–S122. [PubMed: 16501617]

18. ten Berge D, Kurek D, Blauwkamp T, Koole W, Maas A, Eroglu E, Siu RK, Nusse R. Embryonic stem cells require Wnt proteins to prevent differentiation to epiblast stem cells. Nat. Cell Bio. 2011; 13:1070–1075. [PubMed: 21841791]
19. Bottomly D, Kyler SL, McWeeney SK, Yochum GS. Identification of beta-catenin binding regions in colon cancer cells using CHIP-Seq. Nuc. Acids Res. 2010; 38:5735–45.
20. Schuijers J, Mokry M, Hatzis P, Cuppen E, Clevers H. Wnt-induced transcriptional activation is exclusively mediated by TCF/LEF. EMBO J. 2014; 33:146–56. [PubMed: 24413017]
21. Zhang CU, Blauwkamp TA, Burby PE, Cadigan KM. Wnt-mediated reperssion via bipartite DNA recognition by TCF in the *Drosophila* hematopoietic system. PLoS Genet. 2014; 10:e1004509. [PubMed: 25144371]
22. Milo R, Shen-Orr S, Itzkovitz S, Kashtan N, Chklovskii D, Alon U. Network motifs: simple building blocks of complex networks. Science. 2002; 298:824–827. [PubMed: 12399590]
23. Lee TI, Rinaldi NJ, Robert F, Odom DT, Bar-Joseph Z, Gerber GK, Hannett NM, Harbison CT, Thompson CM, Simon I, et al. Transcriptional regulatory networks in *Saccharomyces cerevisiae*. Science. 2002; 298:799–804. [PubMed: 12399584]
24. Boyer LA, Lee TI, Cole MF, Johnstone SE, Levine SS, Zucker JP, Guenther MG, Kumar RM, Murray HL, Jenner RG, et al. Core transcriptional regulatory circuitry in human embryonic stem cells. Cell. 2005; 122:947–956. [PubMed: 16153702]
25. Swiers G, Patient R, Loose M. Genetic regulatory networks programming hematopoietic stem cells and erythroid lineage specification. Dev. Biol. 2006; 294:525–540. [PubMed: 16626682]
26. Egger LA, Park H, Inouye M. Signal transduction via the histidyl-aspartyl phosphorelay. Genes to Cells. 1997; 2(3):167–184. [PubMed: 9189755]
27. Hart Y, Antebi YE, Mayo AE, Friedman N, Alon U. Design principles of cell circuits with paradoxical components. Proceedings of the National Academy of Sciences. 2012; 109(21):8346–8351.
28. Basu S, Mehreja R, Thiberge S, Chen MT, Weiss R. Spatiotemporal control of gene expression with pulse-generating networks. Proc. Natl. Acad. Sci. 2004; 101:6355–6360. [PubMed: 15096621]
29. Mangan S, Alon U. Structure and function of the feed-forward loop network motif. Proc. Natl. Acad. Sci. 2003; 100:11980–11985. [PubMed: 14530388]
30. Mangan S, Itzkovitz S, Zaslaver A, Alon U. The incoherent feed-forward loop accelerates the response-time of the gal system of *Escherichia coli*. J. Mol. Biol. 2006; 356:1073–1081. [PubMed: 16406067]
31. Entus R, Aufderheide B, Sauro HM. Design and implementation of three incoherent feed-forward motif based biological concentration sensors. Syst. Synth. Biol. 2007; 1:119–128. [PubMed: 19003446]
32. Kaplan S, Bren A, Dekel E, Alon U. The incoherent feed-forward loop can generate non-monotonic input functions for genes. Mol. Syst. Biol. 2008; 4:203. [PubMed: 18628744]
33. Kim D, Kwon YK, Cho KH. The biphasic behavior of incoherent feed-forward loops in biomolecular regulatory networks. Bioessays. 2008; 30:1204–1211. [PubMed: 18937374]
34. Goentoro L, Shoval O, Kirschner MW, Alon U. The incoherent feedforward loop can provide fold-change detection in gene regulation. Mol. Cell. 2009; 36:894–899. [PubMed: 20005851]
35. Sive, HL., Grainger, RM., Harland, RM. Early Development of *Xenopus laevis*: A Laboratory Manual, First Edition. Cold Spring Harbor: Cold Spring Harbor Laboratory Press; 2010.
36. Murray, AW. Cell cycle extracts. In: Brian, BK., Peng, HB., editors. Methods in Cell Biology. New York, NY: Elsevier; 1991. p. 581-605.
37. Gagnon KT, Li L, Chu Y, Janowski BA, Corey DR. RNAi factors are present and active in human cell nuclei. Cell Rep. 2014; 6:211–221. [PubMed: 24388755]
38. Cong L, Ran FA, Cox D, Lin S, Baretto R, Habib N, Hsu PD, Wu X, Jiang W, Marraffini LA, Zhang F. Multiplex genome engineering using CRISP/Cas systems. Science. 2013; 339:819–23. [PubMed: 23287718]
39. Workman CT, Yin Y, Corcoran DL, Ideker T, Stormo GD, Benos PV. enoLOGOS: a verstaile web tool for energy normalized sequence logos. Nuc. Acids Res. 2005; 33:W389–392.

40. Ji H, Jiang H, Ma W, Johnson DS, Myers RM, Wong WH. An integrated software system for analyzing ChIP-chip and ChIP-seq data. Nature biotechnology. 2008; 26(11):1293–1300.

41. Jothi R, Cuddapah S, Barski A, Cui K, Zhao K. Genome-wide identification of in vivo protein–DNA binding sites from ChIP-Seq data. Nucleic acids research. 2008; 36(16):5221–5231. [PubMed: 18684996]

42. Kharchenko PV, Tolstorukov MY, Park PJ. Design and analysis of ChIP-seq experiments for DNA-binding proteins. Nature biotechnology. 2008; 26(12):1351–1359.

43. McLeay RC, Bailey TL. Motif enrichment analysis: a unified framework and an evaluation on ChIP data. BMC Bioinformatics. 2010; 11:165–175. [PubMed: 20356413]

44. Grant CE, Bailey TL, Noble WS. FIMO: Scanning for occurrences of a given motif. Bioinformatics. 2011; 27:1017–1018. [PubMed: 21330290]

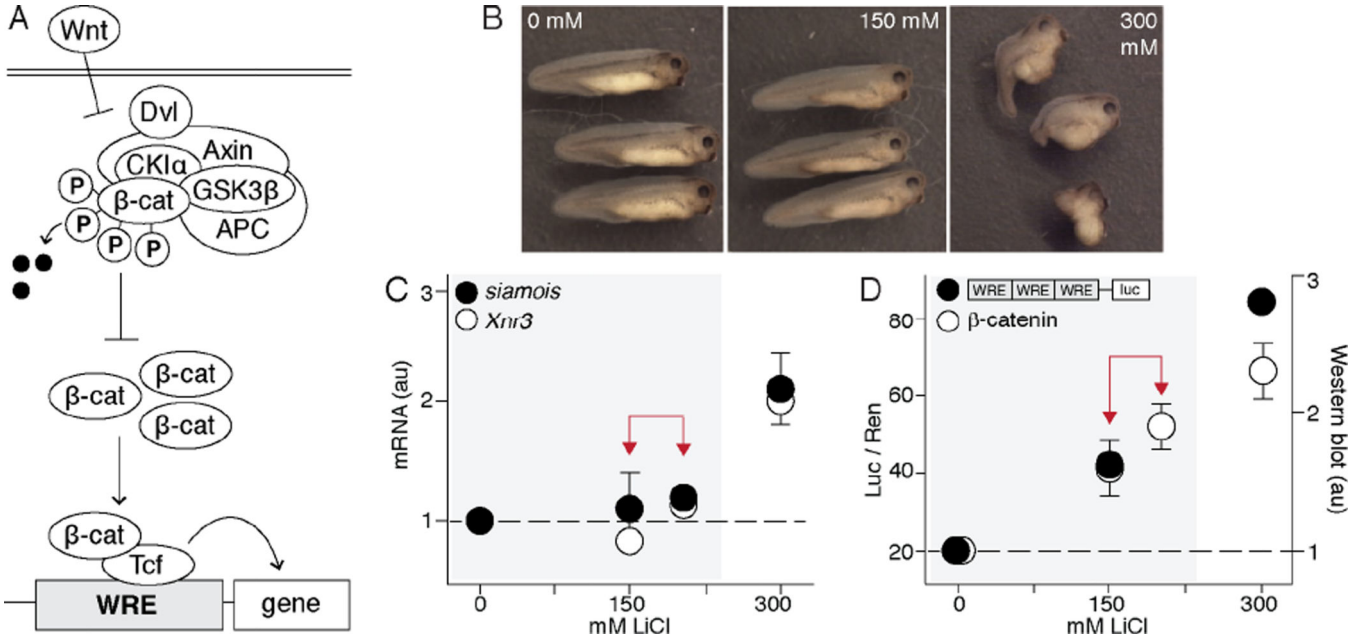

Figure 1. Endogenous genes show regulation not captured by WRE

(A) In the canonical Wnt pathway, Wnt ligand stimulation inhibits the destruction complex, resulting in the accumulation of β-catenin. Together with Tcf/Lef proteins, β-catenin binds to WRE and activate or repress target genes.

(B) *Xenopus* embryos were treated with LiCl for 5 minutes at 32-cell stage, and harvested at stage 10 for qRT-PCR assay, and scored 3–4 days later (shown here).

(C) Expression of target genes, *siamois* (black circle) and *Xnr3* (white circle). Control embryos are untreated sibling embryos. Red arrows highlight how gene expression remains wild type despite perturbations.

(D) Black circle: luciferase/renilla signal from the TopFlash reporter injected at 4-cell stage. White circle: β-catenin level in the embryo measured using Western blot. Red arrows highlight how β-catenin level and TopFlash expression changes with moderate perturbations. Figure B–D are reproduced from [5] with permission. Data are represented as mean ± SEM from 3–5 biological replicates. Error bars not visible have negligible SEM.

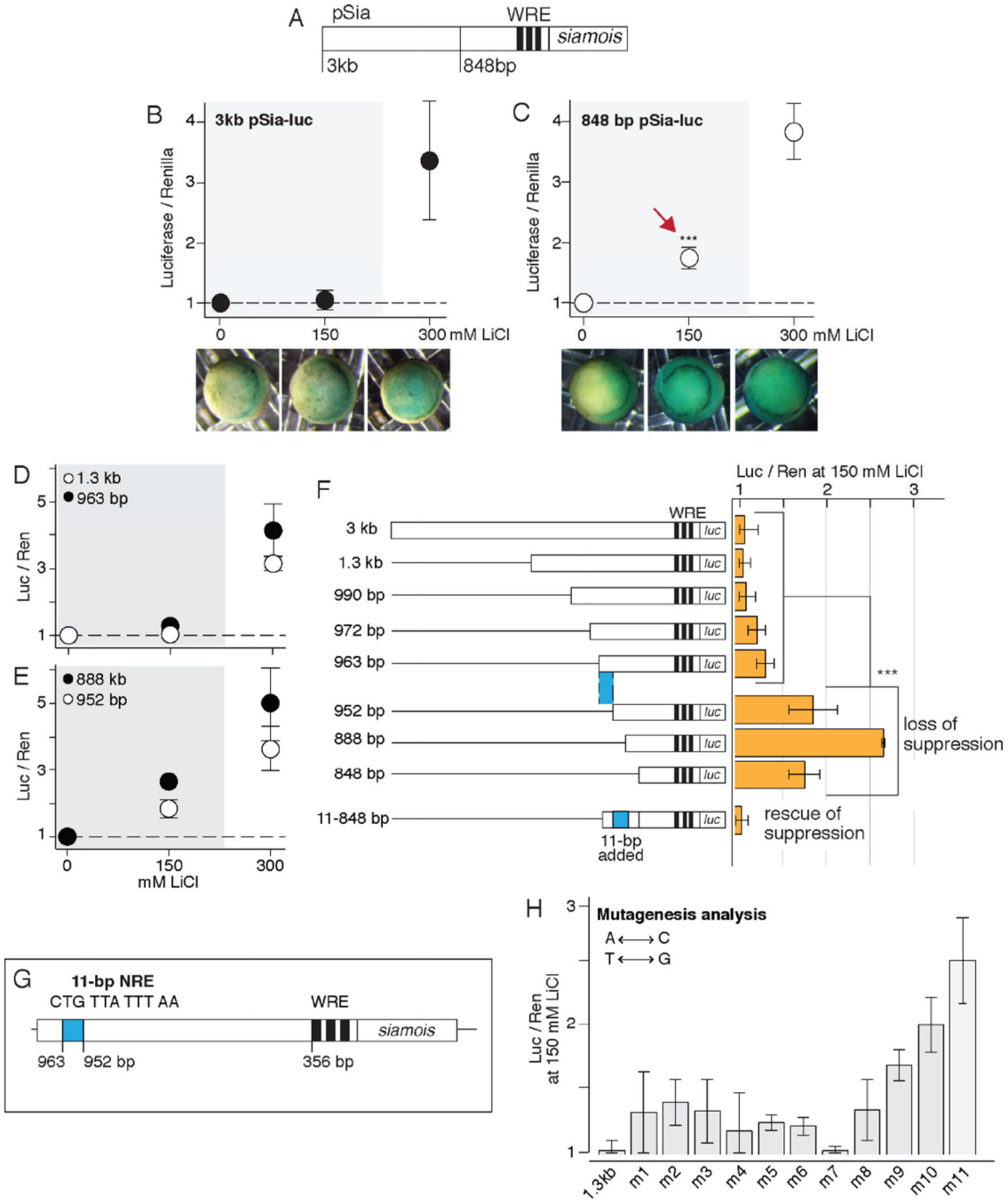

Figure 2. A suppressive 11-bp NRE is necessary for *siamois* regulation

(A) Three WREs (black) are located within 500 bp upstream in *siamois* promoter (pSia) **(B–F, H)** We built luciferase reporters using 3kb and 848bp pSia. The luciferase reporters were injected into each cell at 4-cell stage. Injected embryos were treated with lithium for 5 minutes at 32-cell stage, and harvested for dual-luciferase assay at stage 10. As an injection control, pRL-TK constitutively expressing renilla luciferase was co-injected, and the pSia-driven firefly luciferase signal was measured relative to the renilla luciferase signal. In all the plots shown here, the luciferase/renilla signal is normalized to that in the control,

untreated embryos. Data are presented as mean ± SEM from 3–5 biological replicates. Error bars not visible have negligible SEM.

(B) Expression of 3kb pSia-luc.

(C) Expression of 848bp pSia-luc. p-value = 8.4E-4 (Student's t-test).

Insets below Figure **B** and **C:** *Xenopus* embryos were injected with 3kb or 848bp pSia-LacZ at 4-cell stage, treated with lithium for 5 minutes at 32-cell stage, and fixed at stage 10 for X-Gal staining. In all embryos, dorsal is to the right.

(D) Expression of 1.3kb pSia-luc (black) and 963bp pSia-luc (white).

(E) Expression of 952bp pSia-luc (white) and 888bp pSia-luc (black).

(F) Expression of pSia of various lengths in embryos treated with 150 mM LiCl. p-value = 1.5E–5 (Student's t-test). See also Figure S1.

(G) A suppressive 11-bp NRE (blue) is located between 963 and 952 bp upstream of *siamois*.

(H) Mutagenesis analysis of the 11-bp NRE. Data are mean luciferase/renilla signal ± SEM from 2–4 biological replicates.

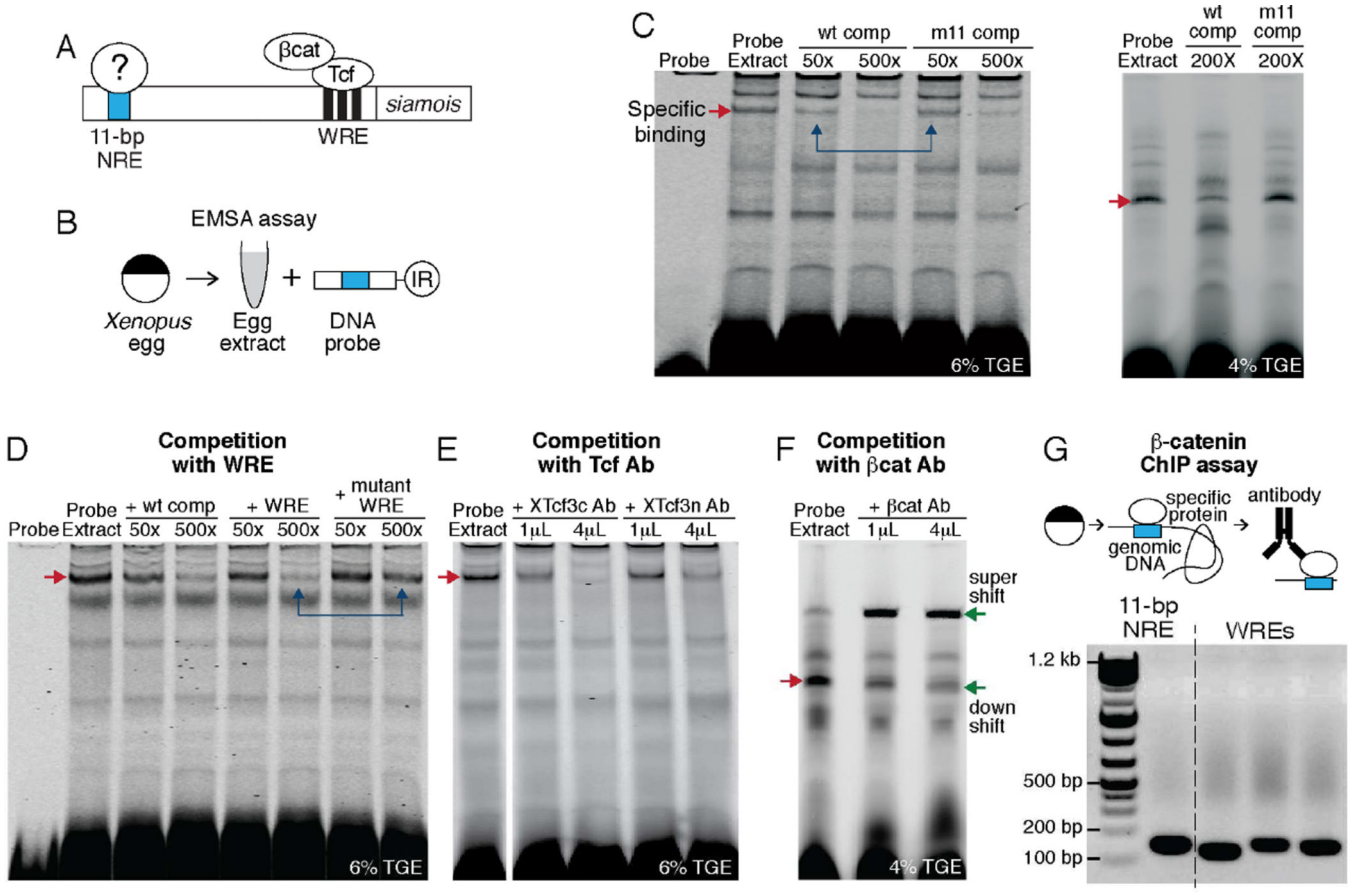

Figure 3. The 11-bp NRE binds to β-catenin and Tcf

(A) We looked for the factor(s) that bind to the 11-bp NRE.

(B) We performed EMSA using *Xenopus* egg extract and a 30-bp probe containing the 11-bp NRE. IR denotes infrared dye used to tag the DNA probe.

(C–F) EMSA analysis. Every panel shown comes from a single gel. Each experiment was repeated 2–4 times. In all gels, red arrow indicates the specific EMSA band.

(C) Left gel: Competition with excess, unlabeled wild-type probe (lanes 3–4) and excess, unlabeled probe containing the m11 mutation (lanes 5–6). Right gel: EMSA using a different batch of *Xenopus* extracts, and resolved using a lower-percentage gel.

(D) Competition with excess, unlabeled wild-type probe (lanes 3–4), WRE probe (lanes 5–6), and mutant WRE probe (lanes 7–8). See also Figure S2A.

(E) Competition with polyclonal XTcf3 antibody against the C-terminal of XTcf3 (XTcf3c, lanes 2–3) and against the N-terminal of XTcf3 (XTcf3n, lanes 4–5).

(F) Competition with polyclonal antibody against β-catenin. Red arrow: the specific EMSA band. Green arrows: a supershift and a smear downshift. See also Figure S2B.

(G) Chromatin immunoprecipitation using β-catenin antibody. Genomic DNA was isolated from stage 10 *Xenopus* embryos, sonicated, and pulled-down with β-catenin antibody. Lane 1: PCR amplification from the 11-bp NRE region. Lanes 2–4: PCR amplification from regions containing WRE in the *siamois* promoter.

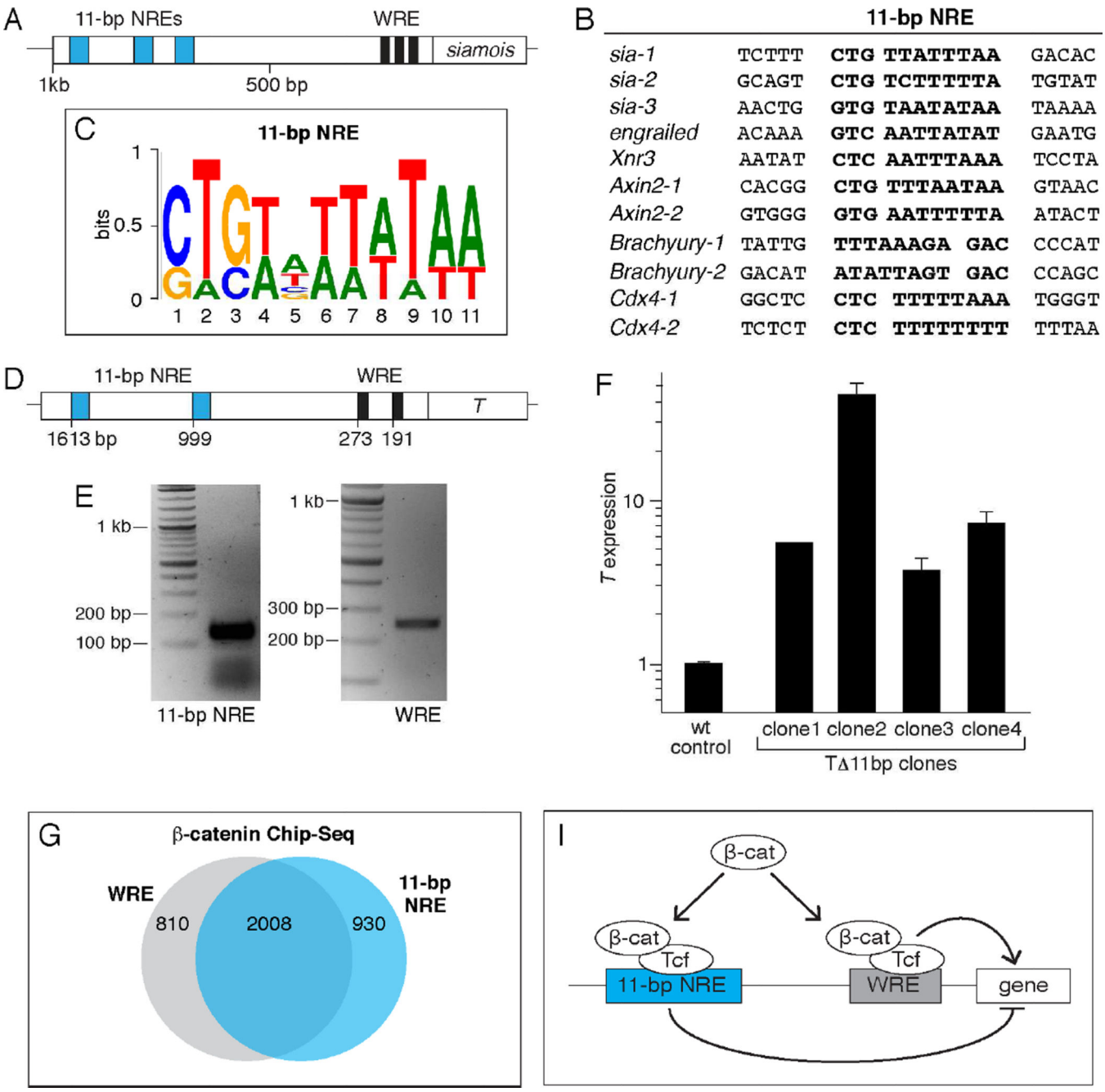

Figure 4. 11-bp NREs regulate *Brachyury* (*T*) in mouse embryonic stem cells

(A) *siamois* promoter contains 3 11-bp NREs, including the distal element characterized so far (blue). See also Figure S3A.

(B) 11-bp NREs found in the promoters of *siamois, engrailed, Xnr3*, *Brachyury*, *Axin2, Cdx4*.

(C) Position frequency matrix built using the identified 11-bp NREs in **(B)**. See also Figure S3B–C.

(D) *T* promoter in mESC contains 2 WREs and 2 predicted 11-bp NREs.

(E) ChIP using β-catenin antibody, followed by PCR amplification from 11-bp NRE (left) and WRE region (right) in the *T* promoter. The result was reproducible across two biological replicates. To ensure that immunoprecipitation of the 11-bp NRE fragments was not confounded by WRE, we sonicated the chromatin to 100–300 bp and performed PCR validation.

(F) Crisp/Cas9 was used to target genomic deletion of the 11-bp NREs in the *T* promoter. Four mESC clones carrying genomic deletion of 11-bp NREs (*T*Δ11bp) were analyzed with qRT-PCR for *T* expression. Error bars indicate SD from 3 biological replicates.

(G) Analysis of β-catenin Chip-Seq on HEK293T cells. We examined 1kb β-catenin peak regions for the presence of the 11-bp NRE and WRE. Out of the 4484 total peaks from the β-catenin Chip-Seq, 3748 contain the 11-bp NRE and/or WRE motifs. Out of these 3748 peaks, 2008 contain both motifs. See also Figure S4.

(H) Our findings suggest that signal in the Wnt pathway does not only activate target genes through WRE, but also tunes expression of the gene through a suppressive 11-bp NRE. Further, our findings also suggest that β-catenin mediates this coupling.